Bactericidal Core–Shell Paramagnetic Nanoparticles Functionalized with Poly(hexamethylene biguanide)

ARTICLE *in* LANGMUIR · JANUARY 2011

Impact Factor: 4.46 · DOI: 10.1021/la1039909 · Source: PubMed

6 AUTHORS, INCLUDING:

Lev Bromberg
Massachusetts Institute of Technology
147 PUBLICATIONS **4,407** CITATIONS
SEE PROFILE

Angel Concheiro
University of Santiago de Compostela
257 PUBLICATIONS **5,022** CITATIONS
SEE PROFILE

Beatriz Magarinos
University of Santiago de Compostela
109 PUBLICATIONS **2,510** CITATIONS
SEE PROFILE

Carmen alvarez-lorenzo
University of Santiago de Compostela
238 PUBLICATIONS **5,322** CITATIONS
SEE PROFILE

Langmuir
Article
pubs.acs.org/Langmuir

Bactericidal Core-Shell Paramagnetic Nanoparticles Functionalized with Poly(hexamethylene biguanide)

Lev Bromberg,[†] Emily P. Chang,[†] T. Alan Hatton,[†] Angel Concheiro,[‡] Beatriz Magariños,[§] and Carmen Alvarez-Lorenzo*,[‡]

[†]*Department of Chemical Engineering, Massachusetts Institute of Technology, Cambridge, Massachusetts 02139, United States,* [‡]*Departamento de Farmacia y Tecnologia Farmaceutica, and* [§]*Departamento de Microbiologia y Parasitologia, Facultad de Biologia, Universidad de Santiago de Compostela, 15782-Santiago de Compostela, Spain*

Received October 4, 2010. Revised Manuscript Received November 18, 2010

Bactericidal paramagnetic particles were obtained either through the attachment of a conjugate of poly(ethyleneimine) (PEI) and poly(hexamethylene biguanide) (PHMBG) to the surface of magnetite (Fe_3O_4) particles, or via the sol-gel encapsulation of magnetite particles with a functional silane (3-glycidoxypropyl trimethoxysilane) and subsequent binding of the polysiloxane shell by the amine/imine groups of PHMBG. The encapsulated core-shell particles possess a high saturation magnetization, which is preserved for more than 10 months while in contact with air in aqueous suspensions. The minimum inhibitory concentration (MIC) of the encapsulated particles for eight types of bacteria was size-dependent, with polydisperse submillimeter particles possessing a several-fold higher MIC than analogous particles sized below 250 nm. The encapsulated particles are biocompatible and nontoxic to mammalian cells such as mouse fibroblasts. The particles efficiently bind both glycopeptide components mimicking the Gram-positive bacteria membranes and whole bacteria, and possess broad-range bactericidal activity. The cell-particle complexes can be captured, manipulated, and removed by means of a magnet.

Introduction

Magnetic nanoparticles consisting of a superparamagnetic core and a functionalized organic shell are attractive for a variety of interdisciplinary technological and biomedical applications.[1,2] The functionalized coating enables selective recognition and capture of specific molecules or organisms, while the paramagnetic properties facilitate a controlled movement toward a target through the action of a magnetic field produced by a permanent magnet or electromagnet.[3] The smaller the size of the core, the larger the surface area for functionalization. Magnetite (Fe_3O_4) and maghemite (γ-Fe_2O_3) are currently the only nontoxic paramagnetic materials acceptable for biomedical applications.[4] Compared to other conventional techniques of bacteria sorting, magnetic beads modified with specific ligands such as haptens enable higher throughput and require less specialized equipment while preserving the cell viability.[5] Nanoparticles modified with glycopeptide antibiotics, such as vancomycin, can be used to selectively trap traces of pathogens from biological fluids.[6−8] The glycopeptide antibiotics are capable of recognizing the cell surfaces of Gram-positive bacteria, and thus, the vancomycin-modified nanoparticles possess a recognition ability through the selective binding to such germs. However, the capturing capacity of the particles depends on the number of vancomycin ligands attached to the particle surface, and the ability of the antibiotic to function depends on the arrangement of the ligands; these conditions complicate the synthetic route and permit recovery of only small traces of the specific bacteria. In the present work, we introduce nonspecific nanoparticles that can be synthesized in large scale quantities without solvent exchange and are capable of capturing and killing a broad range of bacteria. Such magnetic nanoparticles loaded with biocidal substances offer a green and cost-effective approach to the eradication of pathogenic microorganisms from contaminated water sources, aqueous media, and soil.[9,10] Furthermore, they could be an alternative to the widespread use of acriflavine and other antimicrobial agents deposited in water by fish farmers.[11]

We have previously observed that magnetite nanoparticles functionalized with poly(hexamethylene biguanide) (PHMBG) can be captured, together with germs bound to the particle surface, by a high gradient magnetic separation (HGMS) process and that the microorganisms' DNA could be extracted and analyzed by real-time polymerase chain reaction.[12] Importantly, the PHMBG-functionalized particles were able to sequester lipopolysaccharides from Gram-negative bacteria and kill *Escherichia coli* at concentrations significantly lower than those toxic for mammalian cells.[10,12] Therefore, these particles may enable not only in situ biodefense but also the monitoring of the presence of dangerous germs in aqueous habitats.

*To whom correspondence should be addressed. Telephone: 34-881815239, Fax: 34-981547148. E-mail: carmen.alvarez.lorenzo@usc.es.

(1) Pankhurst, Q. A.; Connoly, J.; Jones, S. K.; Dobson, J. *J. Phys. D* **2003**, *36*, R167–R181.
(2) Gao, J.; Gu, H.; Xu, B. *Acc. Chem. Res.* **2009**, *42*, 1097–1107.
(3) Vatta, L. L.; Sanderson, R. D.; Koch, K. R. *Pure Appl. Chem.* **2006**, *78*, 1793–1801.
(4) Müller, R.; Steinmetz, H.; Hiergeist, R.; Gawalek, W. *J. Magn. Magn. Mater.* **2004**, *276*, 272–276.
(5) Porter, J.; Pickup, R. In *Methods in Biotechnology*; Edwards, C., Ed.; Humana Press Inc.: Totowa, NJ, 2010; Vol. *12*.
(6) Lin, Y.-S.; Tsai, P.-J.; Weng, M.-F.; Chen, Y.-C. *Anal. Chem.* **2005**, *77*, 1753–1760.
(7) Li, S.; Guo, Z.; Wu, H. F.; Liu, Y.; Yang, Z.; Woo, C. H. *Anal. Bioanal. Chem.* **2010**, *397*, 2465–2476.
(8) Kell, A. J.; Stewart, G.; Ryan, S.; Peytavi, R.; Boissinot, M.; Huletsky, A.; Bergeron, M. G.; Simard, B. *ACS Nano* **2008**, *2*, 1777–1788.
(9) Ambashta, R. D.; Sillanpää, M. *J. Hazard. Mater.* **2010**, *180*, 38–49.
(10) Bromberg, L.; Chang, E. P.; Alvarez-Lorenzo, C.; Magariños, B.; Concheiro, A.; Hatton, T.A.. *Langmuir* **2010**, *26*, 8829–8835.
(11) Plakas, S. M.; el Said, K. R.; Bencsath, F. A.; Musser, S. M.; Hayton, W. L. *Xenobiotica* **1998**, *28*, 605–616.
(12) Bromberg, L.; Raduyk, S.; Hatton, T. A. *Anal. Chem.* **2009**, *81*, 5637–5645.

To enhance the long-term stability and biocompatibility of the PHMBG-functionalized particles, in the present work we introduce particles with a core-shell structure, where magnetite is encapsulated by a functional polysiloxane prior to functionalization with the biguanide polymer. Such particles demonstrated size-dependent bactericidal properties and were able to efficiently capture *Staphylococcus aureus* cells, as described below.

Experimental Section

Materials. Branched poly(ethyleneimine) (PEI; nominal average molecular weight, 25 kDa) with a molar ratio of primary to secondary to tertiary amino groups of 1:2:1 was obtained from Sigma-Aldrich Chemical Co. (St. Louis, MO). After dialysis in water (MWCO 12−14 kDa) and removal of lower molecular weight fractions, the M_w was 38 kDa and M_w/M_n = 1.55. Poly(hexamethylene biguanide) (PHMBG) was from Arch UK Biocides Ltd. (Manchester, U.K.), supplied as a 20 wt % aqueous solution (Cosmocil CQ) with a reported M_w of 2674 and a polydispersity of 1.89. The solution was dialyzed against deionized water (MWCO 2 kDa) and lyophilized to dryness. After dialysis, the M_w and polydispersity were 2810 and 1.69, respectively. That is, the PHMBG chain on average consisted of 7.3 repeating units. $FeCl_3 \cdot 6H_2O$ (98%), $FeCl_2 \cdot 4H_2O$ (99%), aqueous 25 wt % glutaraldehyde, tetraethyl orthosilicate (99%, TEOS), and 3-glycidoxypropyl trimethoxysilane (97%, GPTMS) were all purchased from Sigma-Aldrich Chemical Co. (St. Louis, MO). Peptide D-Ala-D-Ala-D-Ala labeled with 5-carboxyfluorescein (5-FAM(DA)$_3$) was custom synthesized by BioNova cientifica S.L. (Madrid, Spain). Saline phosphate buffer pH 7.4 (PBS) was prepared with 10 mmol/L Na_2HPO_4, 2 mmol/L KH_2PO_4, 137 mmol/L NaCl, and 2.7 mmol/L KCl and filtered through a 0.45 μm membrane.

Magnetic Particle Synthesis. Poly(hexamethylene biguanide) and polyethyleneimine-modified magnetite (PHMBG-PEI-M) particles were synthesized as previously described.[10] First, PEI-modified magnetite (PEI-M) was synthesized by chemical coprecipitation of iron(II) and (III) chlorides. Namely, 13.52 g (50 mmol) of $FeCl_3.6H_2O$ and 4.97 g (25 mmol) of $FeCl_2.4H_2O$ were added to 200 mL of deionized water, and the solution was deaerated by nitrogen purge in a stirred 250 mL three-necked flask for 0.5 h. The temperature of the flask contents was then brought to 60 °C. An aqueous solution containing PEI (5 g of polymer in 40 mL of water, pH adjusted to 6) and the fluorosurfactant Zonyl 9373 (0.5 g) was added to the flask; the resulting mixture was equilibrated at 80 °C for 15 min while gently stirring under nitrogen purge. Then the nitrogen purge was ceased, and the contents of the flask were at once added to 100 mL of a 28% ammonium hydroxide solution; the mixture, which rapidly turned black, was stirred vigorously for 5−10 min. The resulting precipitate was kept at 90 °C for 1 h and separated from the liquid by decantation using a Franz isodynamic magnetic separator (Trenton, NJ). The precipitate was resuspended in deionized water with sonication, dialyzed against excess deionized water (membrane MWCO 12−14 kDa), and lyophilized. The PEI-M particles (2 g) were suspended in 20 mL of 5 wt % PHMBG aqueous solution with sonication for 30 s. To this suspension, 10 mL of 25% aqueous glutaraldehyde was added, and the resulting suspension was quickly stirred and then shaken at room temperature for 16 h. The resulting suspension was dialyzed against excess DI water (MWCO 12−14 kDa) and lyophilized. The black solids were suspended at 1−2 wt % in deionized water using a Branson sonifier, resulting in a polydisperse particle population designated PHMBG-PEI-M. Elemental analysis: C, 29.0%; H, 6.04%; Fe, 36.6%; N, 14.3%. On average, the particles contained 50−60 wt % polymer and had a hydrodynamic diameter of 50−150 nm and a saturation magnetization of 40−65 emu/g of magnetite.

Magnetite-silica core-shell particles functionalized with PHMBG (PHMBG-M/SiO_2) were synthesized in three consecutive steps (Figure 1). First, magnetite particles were prepared; they were well-dispersed in water with the aid of tetramethylammonium hydroxide (TMAOH). In the second step, the magnetic particles were encapsulated by a shell comprised of tetraethyl orthosilicate (TEOS) and epoxy-functional 3-glycidoxypropyl trimethoxysilane (GPTMS). The third step was the binding of the epoxy groups on the core−shell particle with the amine-imine groups of PHMBG. Depending on the concentration of the particles in the PHMBG grafting step, we obtained PHMBG-M/SiO_2 particles with varying size and biocidal activity. Thus, $FeCl_3 \cdot 6H_2O$ (7.58, 28 mmol) and $FeCl_2 \cdot 4H_2O$ (2.78 g, 14 mmol) were dissolved in 25 mL of deionized water and the solution was brought to 80 °C under nitrogen purge within ~30 min. The solution was poured into 25 mL of 30% NH_4OH, and the resulting black precipitate was stirred and kept at 80 °C for 1 h. The resulting particle suspension was sonicated for 1 min and separated from the supernatant by magnetocollection (magnetic field, ~1.2 T). The particles were then placed into a tube containing 30 mL of 0.33 M aqueous solution of TMAOH. The suspension was observed to be stable. The particles were separated by magnetocollection and washed twice by 50 mL of deionized water each time. The above steps were repeated three times and the resulting TMAOH-stabilized magnetite suspension fractions were combined together (100 mL total, magnetite content, ~30.5 g) and diluted by 100 mL ethanol. Then, 10 mL of TEOS were added and the suspension was sonicated for 5 min, followed by addition of 10 mL of GPTMS. The suspension was kept under vigorous shaking at room temperature for 2 days, after which fractions of the suspension were conjugated with PHMBG in two different modes, resulting in two fractions of particles of varying size. Particles of a broad range of sizes, including submillimeter-sized, were designated PHMBG-M/SiO_2 (t) and were synthesized using 190 mL of the above suspension (magnetite content, 30 g), to which a solution of 15 g of PHMBG in 50 mL of deionized water was added. The mixture was kept at 80 °C for 1 h followed by shaking at 250 rpm at room temperature for 2 days. Then the product was dialyzed against an excess of deionized water (MWCO 12−14 kDa), snap-frozen, and lyophilized. Particles of smaller size, designated PHMBG-M/SiO_2 (s), were synthesized using 10 mL of the above suspension (magnetite content, ~0.5 g), to which a solution of 0.9 g of PHMBG in 500 mL of deionized water was added. The mixture was sonicated for 5 min and kept at 80 °C for 16 h followed by shaking at 250 rpm at room temperature for 2 days. The resulting particles were characterized by elemental analysis, TEM, DLS, SQUID, and TGA. Elemental analysis of PHMBG-M/SiO_2: (i) fraction designated (t): C, 25.4; H, 5.05; Fe, 19.6; N, 18.8%; (ii) fraction designated (s): C, 27.8; H,

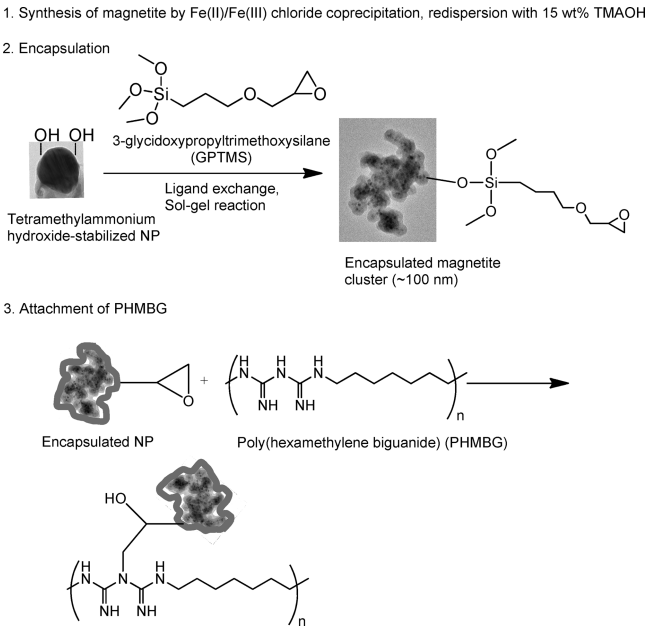

Figure 1. Schematic of the synthesis of PHMBG-M/SiO_2 particles.

5.83; Fe, 18.3; N, 19.7%. The typical size of the PHMBG-M/SiO_2 (s) particles was observed to be approximately 150 nm; the polymer content varied in the range 60−65 wt %, and the saturation magnetization ranged from 80 to 89 emu/g of magnetite.

Particle Characterization Methods. *Transmission Electron Microscopy* (*TEM*). TEM was performed on a JEOL 2010 transmission electron microscope. Samples were prepared by placing drops of the nanoparticle dispersion on carbon-coated 200 mesh copper grids (Electron Microscopy Sciences) and imaged at an accelerating voltage of 200 kV.

Fourier Transform Infrared (*FTIR*) *Spectroscopy*. FTIR spectroscopy was performed on a NEXUS 870 FTIR spectrometer (Thermo Nicolet, Inc.). Spectra were recorded over the wavenumber range between 4000 and 400 cm^{-1} at a resolution of 2 cm^{-1}, and they are reported as the average of 64 spectral scans. All particle samples were dried under vacuum to constant weight, ground and blended with KBr, and pressed to form the pellets used in the measurements.

ζ *Potential Measurements*. The particles were dispersed in 10 mM KCl aqueous solution at approximately 0.05 wt % concentration, and the pH of the nanoparticle suspensions was adjusted by adding 1 M HCl or NaOH aqueous solutions. All ζ potential measurements were performed using a Brookhaven ZetaPALS ζ potential analyzer (Brookhaven Instruments Corporation). The Smoluchowski equation was used to calculate the ζ potential from the electrophoretic mobility. The reported ζ potential values are averages of five measurements, each of which was obtained over 25 electrode cycles.

Dynamic Light Scattering (*DLS*). DLS experiments were performed with a Brookhaven BI-200SM light scattering system (Brookhaven Instruments Corporation) at a measurement angle of 90°. Particles dispersed in aqueous 10 mM KCl (pH adjusted by 1 M NaOH or HCl) were filtered with a 0.45 μm syringe filter prior to the DLS tests. Particle sizes greater than 0.45 μm reported were due to minor reaggregation of the particles during the measurement. Number-average particle size distributions were obtained using the built-in software, and the reported particle mean hydrodynamic diameters are averages of five measurements, each conducted for 3 min.

Thermogravimetric Analysis (*TGA*). TGA was conducted using a Q5000IR thermogravimetric analyzer (TA Instruments, Inc.). Samples were subjected to heating scans (20 °C/min) in a temperature ramp mode.

Superconducting Quantum Interference Device (*SQUID*). SQUID experiments were conducted using a Magnetic Property Measurement System model MPMS-5S (Quantum Design) to determine the magnetization of the particles in an applied magnetic field. All SQUID measurements were performed at 300 K over a 0 to +50 kOe range on samples weighing 3−4 mg.

Particle Stability Testing. Representative samples of the PHMBG-M/SiO_2 (t) and PHMBG-PEI-M particles were tested for chemical stability using cyclic voltammetry (CV) and for paramagnetic properties using SQUID. The CV measurements were performed with a VersaSTAT 3 potentiostat (Princeton Applied Research, Oak Ridge, TN) using a three-electrode microcell assembly (MF 1065, Bioanalytical Systems, Inc., West Lafayette, IN) with a carbon paste working electrode, a platinum wire auxiliary electrode, and a Ag/AgCl reference electrode filled with an aqueous 3 M NaCl solution. The reference electrode adhered to the acceptable range test relative to a standard calomel electrode (SCE). The working electrode was filled with 0.2 g/g of test sample thoroughly mixed and compacted in oil-base carbon paste (BASi CF-1010); the tip of the electrode was polished against filter paper. The electrolyte solution used in the cell was aqueous 0.1 M HCl, and the CV was measured by applying a cyclic potential between −1.5 and 2.0 V versus the Ag/AgCl electrode in five cycles.

SQUID measurements were performed on particle samples at two time points. The first sample was tested for its paramagnetic properties by SQUID and for iron content within 1−2 days after synthesis while being kept under a nitrogen blanket in the dry state. The second sample was placed into excess deionized water equilibrated with air, and the pH was adjusted to 7.4 using an aqueous 0.1 mM NaOH solution. The suspension was kept in sealed tubes at room temperature for about 10 months under periodic rocking at 200 rpm. The tubes were opened once a week and purged for 10−15 min by air bubbling; the pH was checked and readjusted as necessary. A change of color in the aqueous phase of the PHMBG-PEI-M particles suspension upon aging was observed. At the end of the test, the aged suspensions were frozen at −80 °C and lyophilized to dryness. The iron content in the solids was measured by elemental analysis; paramagnetic properties were assessed by SQUID.

Determination of Minimum Inhibitory Concentration (MIC). The following microorganisms were used (American Type Culture Collection, Manassas, VA or La Colección Española de Cultivos Tipo, Valencia, Spain): Gram-positive bacteria *Staphylococcus aureus* ATCC 25923 and ATCC 6538, *Staphylococcus epidermidis* CECT 4184, *Lactococcus lactis* ATCC 7963, *Streptococcus phocae* ATCC51973, and *Lactococcus garvieae* ATCC2155; Gram-negative bacteria *Pseudomonas aeruginosa* CECT 110 and ATCC 15692, *Escherichia coli* ATCC 11229, and *Salmonella enterica* ATCC 13311. The bacteria were grown at 37 °C in Luria-Bertani (LB) broth (Sigma-Aldrich Chemical Co.) (pH 7.3), which was also used for dilutions. The MIC values of PHMBG and the particles were determined in vitro using a broth microdilution assay.[12] The polymer or nanoparticles were dissolved or dispersed, respectively, with brief sonication, into small stock samples of sterile deionized water (10 mL, 3 mg/mL). Serial dilutions between 5 and 300 mg/L final concentration in the liquid medium were dispensed into sterile 96-well polystyrene culture Corning Costar cell plates (Sigma-Aldrich Chemical Co.). The diluted samples were inoculated with a suspension of the test bacterium on the liquid medium to a final concentration of approximately 10^4 CFU/mL. The MIC was defined as the lowest concentration of PHMBG polymer, PHMBG-PEI-M, or PHMBG-M/SiO_2 particles that inhibited bacterial growth after 0.5 h at 37 °C. Measurements were conducted in triplicate. The precision of the MIC values was limited by the dilution factor and was estimated to be ±5 mg/L. Negative control experiments were conducted with the dilutions without bactericidal additives, and no reduction in bacterial counts after 24 h was observed.

A second broth microdilution assay[13] was also utilized. In brief, 100 μL of 10^9 CFU/mL of the bacteria suspensions in PBS pH 7.4 was placed in duplicate in a 96-well plate where 100 μL of PHMBG solution or magnetic particle suspension had been previously added. The concentration of magnetic particles in the wells ranged from 2.5×10^{-7} to 50 mg/mL. Control wells containing only the bacteria or magnetic particle suspensions were also prepared. The plates were incubated at 37 °C for 24 h, and the growth of microorganisms in the wells was verified by seeding them onto trypticase soy agar (TSA) plates.

Disc Diffusion Susceptibility Tests. The bacteria were cultured on TSA plates and incubated at 37 °C for 24 h. Then, the microorganisms were removed from the isolation medium and suspended in PBS pH 7.4 to a final concentration equivalent to the McFarland scale No. 4. Microorganisms were seeded onto TSA plates at a concentration level of 10^9 CFU/mL. Sterile paper discs (6 mm diameter) embedded (20 μL) with 100 mg/mL PHMBG solution or magnetic particle suspension in phosphate buffer pH 7.4 were deposited on TSA plates previously seeded with the bacteria, and then the plates were incubated at 37 °C for 24 h. The inhibition zone was read twice at perpendicular directions, and results yielded the inhibition zone diameter. Inhibition zones of < 6 mm indicate no antibacterial activity.

Binding of Model Peptide to Magnetic Particles. The fluorescence was recorded using a FLUOstar Optima Microplate

(13) National Committee for Clinical Laboratory Standards. CLSI document M07-A8. Methods for Dilution Antimicrobial Susceptibility Tests for Bacteria That Grow Aerobically; Approved Standard-Eighth ed.. Clinical and Laboratory Standards Institute, Wayne, PA, 2009.

Fluorometer (BMG LABTECH GmbH, Germany) fitted with 485 nm excitation and 520 nm emission filters. To establish the kinetics of the peptide-particle binding, PHMBG-PEI-M or PHMBG-M/SiO_2 particles (1 or 3 mg) were added to Eppendorf Lobind tubes containing 1 mL solution of 5-FAM$(DA)_3$ (2.97×10^{-5} M) in PBS and briefly vortexed. The fluorescence intensity at 520 nm was monitored at different time intervals for 90 min. The magnetic particles were collected at the bottom of the tube with the use of an external magnetic stir bar retriever and 150 μL of the supernatant solution was carefully removed and placed into wells of a 96-well plate. After each fluorescence measurement, the samples were immediately returned to the tubes, which were again agitated to ensure homogeneous distribution of the particles.

The kinetics of the 5-FAM$(DA)_3$ binding to the PHMBG-modified particles appeared to be very fast (Supporting Information Figure S1). Once PHMBG-PEI-M particles were added to the 5-FAM$(DA)_3$ solution, the fluorescence signal immediately decreased and stabilized in less than 10 min, for either concentration of the particles tested (1 or 3 mg/mL). Similar results were observed with the PHMBG-M/SiO_2 (t) particles. Hence, an equilibration time of 15 min was chosen to measure the equilibrium binding of the probe to the particles in the subsequent experiments.

The peptide adsorption isotherms were measured at 25 °C as follows. PHMBG-PEI-M or PHMBG-M/SiO_2 (t) particles (1.3 mg) were added to Eppendorf Lobind tubes containing 1.8 mL of 5-FAM$(DA)_3$ solutions in PBS with the peptide concentrations ranging from 9.28×10^{-8} to 2.97×10^{-5} M. The tubes were agitated for 15 min. Then, the magnetic particles were collected at the bottom of the tubes and the fluorescence of the supernatant was recorded as described above. The equilibrium adsorption capacity of the particles (Γ, mol/g) was found from the following expression:[14]

$$\Gamma = \frac{I_0 - I_t}{I_0} \frac{C_p^0}{C_{NP}}$$

where I_0 and I_t are the fluorescence intensities measured before and after particle equilibration with the 5-FAM$(DA)_3$ peptide, respectively, C_p^0 (mol/L) is the initial peptide concentration, and C_{NP} is the nanoparticle concentration in g/L.

Bacteria Binding to the Particles. *S. aureus* (ATCC 6538) cultures were inoculated from stock cultures on tryptic soy agar slants into 100 mL of tryptic soy broth and incubated at 35 °C for 10−12 h. The cultures were harvested by centrifugation at 16 000*g* for 10 min, and the cells were washed once, suspended, and diluted to the desired cell concentrations with the sterile-filtered Hank's balanced salt solution (HBS, pH 7.4, Sigma-Aldrich Chemical Co.). They were cultured until the mid-logarithmic phase of growth ($A_{600} = 0.3$) prior to exposure to the paramagnetic particles. Suspensions of bacterial colonies (1.5×10^6 CFU/mL, 1 mL) were mixed, with brief vortexing, in a conical 2 mL centrifuge tube containing 1 mL of HBS buffer or paramagnetic particles suspension of a known concentration in the same buffer. The nanoparticle suspensions were briefly sonicated just prior to the cell addition. The mixed suspensions were incubated at 37 °C for 3 h with gentle shaking, and the *S. aureus* cells bound to the magnetic particles were separated by placing the tube on top of a $5 \times 5 \times 5$ mm^3 NdFeB, grade N52 magnet (nominal surface field, 5754 G, K&J Magnetics, Inc.) in a vertical position for 0.5 h. The cells collected on the tube's bottom were concentrated by careful pipetting of the supernatant. The isolated NP-cell aggregates were washed with 50 mM Tris-HCl buffer (200 μL × 3), resuspended in 20 mL of the same buffer, and subjected to the concentration determination by flow cytometry using bis-(1,3-dibutylbarbituric acid)trimethine oxonol (DiBAC4(3) stain, Molecular Probes, Inc., a division of Invitrogen) as described elsewhere.[15] DiBAC4(3) stock solution was prepared in 70% ethanol at a concentration of 1 mg/mL and stored at −20 °C. The dye was added directly to the liquid sample to give a final concentration of 1 μg/mL. The samples were incubated for 2 min at room temperature before flow cytometric analysis. The same concentration determination assay was applied to the suspension of bacterial colonies just prior to their contact with the magnetic nanoparticles. The stain binds to both live and dead cells. The capture efficiency was calculated as follows: capture efficiency = $100 \times \text{count}_2/\text{count}_1$, where count_1 and count_2 are the absolute cell counts/mL in samples before and after capture by magnetic nanoparticles; the count values are adjusted for dilutions.

A second fluorimetric assay was applied to determine the binding of magnetic particles to *S. aureus* (ATCC 25923). Magnetic particles (1.3 mg) were incubated with 0.9 mL of a *S. aureus* (2×10^9 cells/mL) suspension in phosphate-buffered saline (pH 7.4) for 15 min at room temperature. Then, the particles were collected at the bottom of the tube with the use of an external magnetic stir bar retriever, and the bacterial suspension was removed by pipetting. The particles were immediately reincubated with 5-FAM$(DA)_3$ solution (4.95×10^{-6} M; 1.8 mL) for 15 min. The particles were moved to the bottom of the tube, and 150 μL of the supernatant solution was carefully removed and placed into wells of a 96-well plate. The fluorescence intensity was measured at 520 nm. A control experiment was performed by incubating the particles directly with 5-FAM$(DA)_3$ solution (4.95×10^{-6} M).

Nanoparticle Cytotoxicity Assay. Cell line L929 (ATCC CCL-1) derived from normal subcutaneous areolar and adipose tissue of a male C3H/An mouse (Sigma-Aldrich) was used for evaluation of the nanoparticle cytotoxicity.[12] The cells were grown without addition of antibiotics in Eagle's minimum essential medium supplemented by 10% fetal bovine serum (FBS, Invitrogen Corp). The MTT cytotoxicity assays (Mosmann's test) were performed as follows. The L929 cells were seeded onto 96-well cell culture plates, 0.1 mL/well, at a density of 1×10^6 cells/mL to reach > 80% confluence. At 24 h after seeding, 0.1 mL of fresh medium and known concentrations of the PHMBG solution or particle suspension pre-equilibrated at 37 °C in the cell medium were added. Six replicate wells per concentration were tested. After 30 min of incubation in a humidified atmosphere of 5% CO_2/95% air at 37 °C, the medium was removed and the wells were washed twice for 2−3 min with 0.2 mL of the fresh medium. Then, the fresh medium containing 0.5 mg of MTT (0.1 mL) was added at 37 °C and kept in the wells for 4 h. The yellow tetrazolium salt is reduced in viable cells to a blue formazan product. After incubation, the media were completely removed, and only cells with the NR medium were washed carefully with two washes of PBS (0.25 mL) for 3 min. Incorporated NR dye was extracted by adding 0.2 mL of 1% (v/v) acetic acid/50% (v/v) ethanol, and the blue formazan product was dissolved in 0.2 mL of 0.04 M HCl in 2-propanol. The plates were agitated on an orbital shaker for at least 1 h in order to ensure quantitative extraction and dissolution of the dyes. The optical density of each well was measured spectrophotometrically at 570 nm using a Bio-Rad Benchmark Plus microplate reader (Bio-Rad Laboratories, Hercules, CA), and the data were normalized by subtracting the background absorbance at 655 nm. In the control experiments, particle dispersions were shown not to interfere with the absorbance readings at $\lambda > 550$ nm. The results were expressed as a percentage of the viability versus control (L929 cells not exposed to the test solution or dispersion). The inferred percentage viability based on the MTT reading for each concentration was used to establish log dose−response curves. The IC_{50} value was defined as the concentration allowing 50% survival of cells and was determined graphically from the log dose−response calibration curves. All experiments were performed three times in the independent measurements. The Student's *t* statistical test (unpaired *t*-test) was used for statistical calculations with a Systat 12 program (Systat Software, Inc.). Probabilities of correlation using Pearson's coefficient (*p*) considered *p* values below 0.05 as a statistically significant threshold.

***S. aureus* Reduction Factor Test.** *S. aureus* (ATCC 6538) cells were maintained on Trypticase soy agar and were incubated

(14) Piyasena, M. E.; Real, L. J.; Diamond, R. A.; Xu, H. H.; Gomez, F. G. *Anal. Bioanal. Chem.* **2008**, *392*, 877–886.
(15) Haidinger, W.; Szostak, M. P.; Jechlinger, W.; Lubitz, W. *Appl. Environ. Microbiol.* **2003**, *69*, 468–474.

under aerobic conditions at 35 °C for 24−48 h. The bacterial suspensions were freshly prepared in sterile distilled water before each experiment. The reduction factor test was performed as described previously[16] and was a part of the particle biocompatibility evaluation. Briefly, 1 mL of PHMBG solution, particle suspension, or sterile distilled water (used to establish the harmlessness of the neutralizing medium) was added to 9 mL of neutralizing medium consisting of Trypticase soy broth containing 3% Tween 80, 3% saponin, 0.1% histidine, and 0.1% cysteine (TSHC). After 10 min of contact, 1 mL of a bacterial suspension adjusted to 10^3 CFU/mL was added. After vortexing, 1 mL of each mixture was placed in duplicate on Trypticase soy agar medium, and the plates were incubated under aerobic conditions. The neutralizing medium allowed for at least 80% of the microorganisms to be recovered. The THSC inactivates biguanides such as PHMBG without any inhibitory effect on bacterial growth.[12] The bactericidal efficiencies were evaluated as follows. An *S. aureus* suspension (1 mL) adjusted to 10^8 CFU/mL was added to 9 mL of each dilution of the PHMBG or particle suspension. After 10 min of contact at 20 °C, 1 mL of each mixture was transferred to 9 mL of neutralizing medium and allowed to remain in contact for 10 min after vortexing. In the case of paramagnetic particles, the latter were separated from the supernatant by magnetocollection using a 5 × 5 × 5 mm NdFeB, grade N52 magnet. Viable bacterial counts were determined by triplicate inclusion of serial dilutions of supernatant samples in Trypticase soy agar. The CFU of the test microorganisms were counted using a Quebec Darkfield colony counter (Reichert Analytical Instruments, Depew, NY) after 48 h of incubation at 37 °C. The $\log_{10}$-reduction factor (rf) for the contact time was calculated according to the formula: $\mathrm{rf} = \log_{10} n_c - \log_{10} n_d$, where n_c is the number of viable cells (CFU) in the inoculum in the presence of phosphate-buffered saline and n_d is the number of viable cells (CFU) in the inoculum after contact with the polymer or nanoparticles. All experiments were repeated three times, and statistically significant mean values of the concentration (C_{3rf}) of additives corresponding to three-$\log_{10}$ reduction (i.e., 99.9% of microorganism killing, rf = 3) are reported herein.

Results and Discussion

Particle Properties. In this work, we introduce core-shell paramagnetic particles with magnetite cores encapsulated by a functional polysiloxane, onto which the biocidal polymer, PHMBG, is covalently attached. For comparison, we used PHMBG-PEI-M particles described previously.[10,12] The PHMBG-PEI-M particles are potent biocides synthesized by coprecipitation of iron(II) and (III) chlorides by ammonia, followed by the coating of the magnetite cores with branched PEI, which is conjugated with PHMBG via linking of the amino groups of PEI with the amino/imino groups of PHMBG by glutaraldehyde. In the PHMBG-PEI-M particles, the amino and imino groups of PEI are chelated directly to the iron ions of magnetite. The PHMBG chains are exposed to the exterior of the nanoparticle clusters.[12] The strong complexation between branched PEI and/or biguanide groups of PHMBG and the Fe^{3+}/Fe^{2+} ions on the magnetite surface leads to formation of water-soluble complexes of PEI and iron ions and, hence, to a gradual dissolution of the magnetite crystals, which can result in the loss by the particles of their paramagnetic properties over time. Mineral dissolution by strong ligands is a well-known phenomenon.[17] As our concept of in situ biodefense involves the long-term presence of the biocides in water,[12] the rationale for the encapsulation step and the core-shell structure herein was the potential to protect the magnetite particles from dissolution and oxidation, which would diminish paramagnetic properties, when exposed to water and air for extended periods of time.

The core-shell particles denoted here as PHMBG-M/SiO_2 were prepared by encapsulating the magnetic cores with a shell consisting of TEOS and epoxy-functional GPTMS that underwent a polycondensation reaction using a modified Stöber method (Figure 1).[18−20] The primary magnetite particles stabilized by tetramethylammonium hydroxide in the first step of the synthetic route (Supporting Information Figure S2) were 6−10 nm and clustered together due to the sol-gel polycondensation of the silicate (TEOS) and silane (GPTMS) around several particles; the silica-coated clusters were 100−150 nm in size (Supporting Information Figure S3). High resolution TEM images suggest that the primary magnetite particles in the clusters were separated by thin siloxane layers. It has been shown that structures in which there is no direct contact between nanoparticles possess high magnetic moments and saturation magnetizations.[19] FTIR spectra of the encapsulated magnetite particles indicated the presence of epoxy and siloxane groups (Supporting Information Figure S4). The epoxy groups on the surface of the encapsulated magnetite were reacted with the amine-imine groups of PHMBG (Figure 1). Because of the multifunctionality of both PHMBG (amino groups) and the particles (epoxy groups), the PHMBG conjugation step resulted in gel-like particles of significantly different sizes, albeit similar chemical composition, depending on the particle and PHMBG concentrations (see the Experimental Section). Larger particle and polymer concentrations result in a higher probability of cross-linking and gel formation. Thus, conjugation conducted in a suspension containing 12 and 6 wt % of magnetite and PHMBG, respectively, resulted in PHMBG-M/SiO_2 (t) particles with sizes ranging from about 100 nm to 500 μm, where the majority of the particles consisted of clustered, encapsulated magnetite bound to other clusters by PHMBG chains. Only approximately 1−3 wt % of the PHMBG-M/SiO_2 (t) particles could permeate through a cellulose acetate membrane with a pore diameter of 0.45 μm using a syringe filter. On the other hand, synthesis in a suspension containing 1 and 1.8 wt % of magnetite and PHMBG, respectively, resulted PHMBG-M/SiO_2 (s) particles, where the majority had number-average diameters below 250 nm (Supporting Information Figure S5). No significant retention of such particles was observed upon filtration through a cellulose acetate membrane with a pore diameter of 0.45 μm. When lyophilized and resuspended, the particles retained their small size. For optimization of the particle synthesis, one needs to consider the ease of scale-up and a high yield for the larger, cross-linked particles versus a low yield for the smaller particles. The TEM images (Figure 2) show that the PHMBG-M/SiO_2 (s) particles are single clusters of magnetite particles (~10 nm) held together by the silica coating, whereas PHMBG-M/SiO_2 (t) particles are gels containing nanoparticle clusters. The magnetite crystal lattice is discernible in Figure 2a, with the average lattice spacings of 0.472 nm, which agrees with the spacings for the {111} plane of magnetite.[21]

Particle Stability. The chemical stability was tested using CV measurements (Figure 3) and SQUID (Figure 4). The CV measurements confirmed the chemical stability of encapsulated PHMBG-M/SiO2 (t) particles against redox reactions and dissolution (Figure 3a). Placing the encapsulated particles, either fresh or aged for 10 months,

(16) Campanac, C.; Pineau, L.; Payard, A.; Baziard-Mouysset, G.; Roques, C. *Antimicrob. Agents Chemother.* **2002**, *46*, 1469–1474.
(17) Norn, K.; Loring, J. S.; Bargar, J. R.; Persson, P. *J. Phys. Chem. C* **2009**, *113*, 7762–7771.
(18) Stöber, W.; Fink, A.; Bohn, E. *J. Colloid Interface Sci.* **1968**, *26*, 62–69.
(19) Barnakov, Y. A.; Yu, M. H.; Rosenzweig, Z. *Langmuir* **2005**, *21*, 7524–7527.
(20) Durdureanu-Angheluta, A.; Stoica, I.; Pinteala, M.; Pricop, L.; Doroftei, F.; Harabagiu, V.; Simionescu, B. C.; Chiriac, H. *High Perform. Polym.* **2009**, *21*, 548–561.
(21) Mann, S.; Moench, T. T.; Williams, R. J. P. *Proc. R. Soc. B* **1984**, *221*, 385–393.

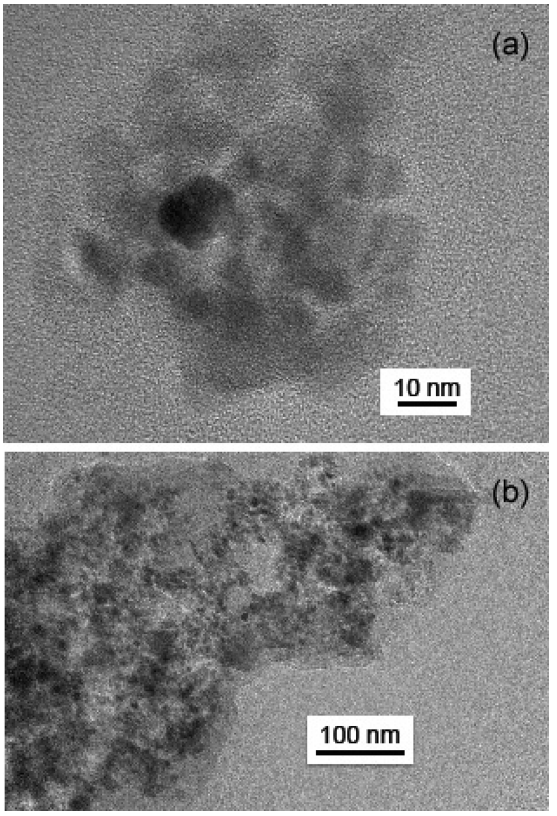

Figure 2. Representative TEM images of (a) PHMBG-M/SiO_2 (s) and (b) PHMBG-M/SiO_2 (t) particles.

in the aggressive electrolyte (0.1 M HCl) did not generate any appreciable background current or electrode peaks characteristic of redox reactions of iron(III) and iron(II) species, indicating that virtually no iron ions were present on the particle surfaces and that the magnetite core was protected by the silica layers. Somewhat similar results have been observed with magnetite encapsulated by TEOS and amine-functionalized silanes such as aminopropyltrimethoxysilane and others.[22] Compared to that reported synthetic route,[22] our synthesis essentially used a one-step method of encapsulation, without the need to exchange water-immiscible organic and aqueous solvents. The electrochemical behavior of the PHMBG-PEI-M particles was strikingly different from that of the encapsulated particles (Figure 3b) in that the former particles were electroactive (generated current on the order of ~800-fold larger than their encapsulated counterparts) and exhibited current peaks.

The anodic peaks at approximately +0.6, +0.8, and +1.2 V in the first cycle of voltammograms of the PHMBG-PEI-M particles correspond to the oxidation of Fe(II) species:[23] $Fe^{2+} \rightarrow Fe^{3+} + e$. The cathodic peaks at 0.15−0.25 V correspond to the Fe(III) reduction: $Fe^{3+} + e \rightarrow Fe^{2+}$. Anodic peaks in the −1 to −0.5 V area are of specific interest, as they describe the reductive dissolution behavior of the iron oxides:[24−26]

$$Fe_3O_4(s) + 8H^+ + 2e \rightarrow 3Fe^{2+} + 4H_2O \text{ for magnetite}$$

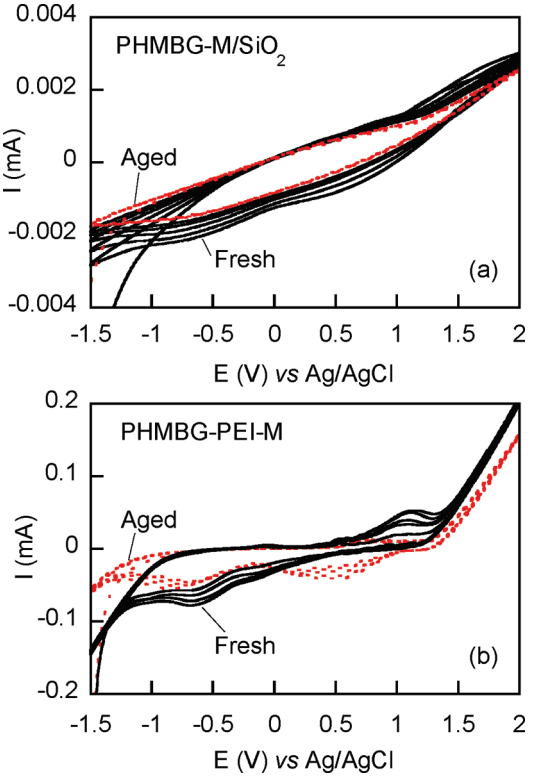

Figure 3. Cyclic voltammetry of PHMBG-M/SiO_2 (a) and PHMBG-PEI-M (b) particles in 0.1 M HCl. Fresh and aged samples are shown by solid and dotted lines, respectively.

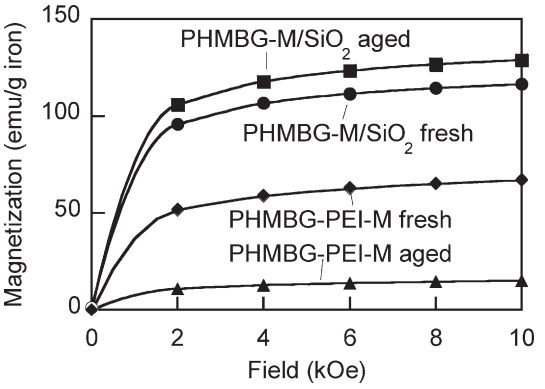

Figure 4. Typical magnetization versus applied magnetic field for PHMBG-M/SiO_2 (t) and PHMBG-PEI-M particles. $T = 300$ K. The field is shown up to 10 kOe, but in some experiments it varied from 0 to 50 kOe. The data collected for increasing and decreasing field overlapped because the material was superparamagnetic. The magnetization is presented in emu per gram of iron. The Fe content of each type of particles was measured by elemental analysis to be 19.0, 19.6, 36.6, and 37.9 wt % in PHMBG-M/SiO_2 fresh, PHMBG-M/SiO_2 aged, PHMBG-PEI-M fresh, and PHMBG-PEI-M aged particles, respectively.

and

$$Fe_2O_3(s) + 6H^+ + 2e \rightarrow 2Fe^{2+} + 2H_2O \text{ for maghemite}$$

The cathodic peaks in the first potential scan with PHMBG-PEI-M appeared at −0.88 and −0.67 V for fresh and aged particles, respectively. The differences between the cathodic peaks due to aging are hard to ascertain quantitatively because both magnetite and other iron oxides and hydroxyoxides can be present in the aged sample. Cathodic peaks in the −0.93 to −0.88 V range attributed

(22) Kang, K.; Choi, J.; Nam, J. H.; Lee, S. C.; Kim, K. J.; Lee, S. W.; Chang, J. H. *J. Phys. Chem. B* **2009**, *113*, 536–543.
(23) Lorenzo, L.; Encinas, P.; Tacsón, M. L.; Vázquez, M. D.; de Francisco, C.; Sánchez-Batanero, P. *J. Solid State Electrochem.* **1991**, *1*, 232–240.
(24) Grygar, T.; Subrt, J.; Bohácek, J. *Collect. Czech. Chem. Commun.* **1995**, *60*, 950–959.
(25) Grygar, T. *Collect. Czech. Chem. Commun.* **1995**, *60*, 1261–1273.
(26) van Oorschot, I. H. M.; Grygar, T.; Dekkers, M. J. *Earth Planet. Sci. Lett.* **2001**, *193*, 631–642.

to the reductive dissolution of magnetite have been reported by Grygar et al.,[24] and their exact position depends on the particle size. From the changes in the reductive dissolution pattern of the aged PHMBG-PEI-M particles, it can be predicted that the aged particles possess a lower saturation magnetization, as all iron oxide/hydroxyoxide species possess a lower magnetization than that of magnetite.

SQUID tests were conducted along with the CV measurements. Both freshly synthesized and aged (kept in water, pH 7.4, for 10 months in the presence of air) samples of PHMBG-M/SiO_2 (t) and PHMBG-PEI-M particles were tested. As shown in Figure 4, the SQUID measurements in the increasing and decreasing magnetic field overlapped, indicating that the particles were superparamagnetic in all cases. The PHMBG-M/SiO_2 particles maintained their high saturation magnetization, on the order of 125−135 emu/g of iron (i.e., 80−90 emu/g of magnetite), throughout the test. The saturation magnetization of bulk magnetite has been reported to be 92 emu/g.[27] In contrast, the saturation magnetization of the PHMBG-PEI-M particles declined from approximately 80 to 18 emu/g of iron after prolonged storage in water in the presence of air. The lower magnetizations of fresh PHMBG-PEI-M particles are due to the significant volume fraction of the polymers and the existence of a well-developed polymer−metal ion surface layer with reduced magnetization on the individual nanoparticles.[12] Therefore, the creation of the siloxane layer around individual magnetite particles in PHMBG-M/SiO_2 (Figure 2) reduces the direct binding of the polymer to the magnetite surface and thus enhances the saturation magnetization. Because the PHMBG-PEI-M particles lacked this layer, the aging and oxidation of magnetite into maghemite and possibly to iron oxyhydroxides in the presence of air and amines in an aqueous environment reduced their overall magnetization. Overall, the encapsulation described herein dramatically enhanced the chemical stability of the paramagnetic particles.

Bacteria Binding, Manipulation, and Removal Using Paramagnetic Particles. PHMBG polymer has a pK_a of 11 as well as multiple hydrophobic hexamethylene groups,[10,12] and thus, the PHMBG-modified magnetite particles are strong cation exchangers, capable of nonspecific binding to anionic lipids in bacterial membranes.[10,12] The PHMBG-M/SiO_2 (t), PHMBG-M/SiO_2 (s), and PHMBG-PEI-M particles of the present study were characterized by ζ potentials of 29.8 ± 1.68, 34.5 ± 1.34, and 37.8 ± 1.11 mV, respectively, in aqueous 10 mM KCl at 25 °C. While binding to the lipopolysaccharides (LPS), the prominent structural component of the outer membrane of Gram-negative bacteria, dominates the bactericidal action against these microorganisms,[10] in the present work we were primarily interested in explaining the action of our particles against Gram-positive bacteria, taking *S. aureus* as a representative example. The outer surface of the *S. aureus* membrane is rich in repeating units of peptidoglycans (PG); each PG unit consists of a disaccharide (*N*-acetylglucosamine and *N*-acetylmuramic acid), a pentapeptide chain (L-Ala-D-*iso*-Gln-L-Lys-D-Ala-D-Ala), and an attached pentaglycyl bridging segment.[28] The interactions between antibiotics and various probes and Gram-positive bacteria are frequently modeled by the probe binding to the terminal D-Ala-D-Ala dipeptide.[14,29] In the present work, we followed this trend using a D-Ala-D-Ala-D-Ala tripeptide labeled with 5-carboxyfluorescein (5-FAM(DA)$_3$) as a model component of the bacterial membrane.

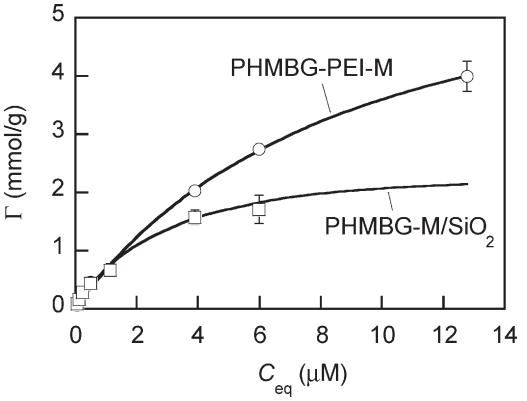

Figure 5. Binding isotherms of 5-FAM(DA)$_3$ per weight of PHMBG-PEI-M and PHMBG-M/SiO_2 particles versus concentration of 5-FAM(DA)$_3$ in solution equilibrated with the particles (C_{eq}). Solid lines represent fits to the Langmuir equation.

The equilibrium adsorption isotherms of 5-FAM(DA)$_3$ onto the particles are depicted in Figure 5. Solid lines represent fits to the Langmuir equation $\Gamma = \Gamma_{max}KC_{eq}/(1 + KC_{eq})$, where Γ_{max} (mmol/g) is the adsorption capacity and K (μmol/L) is the equilibrium constant. The computation was performed by varying Γ_{max} and K to minimize differences with experimental data using MATLAB software. The obtained plateau adsorption capacities of the PHMBG-M/SiO_2 (t) and PHMBG-PEI-M particles were 2.6 and 6.8 mmol/g, respectively. Based on elemental analysis and structure modeling, the content of biguanide groups in the PHMBG-M/SiO_2 (t) and PHMBG-PEI-M particles is approximately 2.3 mmol/g and 1.2 mmol/g, respectively, but the latter particles also possess ca. 3.5 mmol/g of amino groups from PEI. Considering that each biguanide moiety contains several amino/imino groups, each of which can act as a binding site for the terminal carboxyl group of 5-FAM(DA)$_3$, we can conclude that the particle capacity found from the peptide adsorption isotherms was close to the total content of cationic ion-exchange groups. It interesting to compare these results with the PHMBG-PEI-M particle binding to DNA of high molecular weight that we reported previously.[10] At saturation, one phosphate group of DNA is bound to one in 40−50 of the cationic amino and/or biguanide groups on the nanoparticles. Unlike the DNA, a small probe such as 5-FAM(DA)$_3$ is not sterically constrained and appears to be able to bind almost any cationic group available on the surface of the nanoparticles.

The ability of the magnetic particles to bind *S. aureus* cells was qualified by the competitive displacement with 5-FAM(DA)$_3$. A given amount of particles was incubated with a fixed concentration of *S. aureus* and then transferred to the 5-FAM(DA)$_3$ solution. Upon binding of the *S. aureus* cells onto the particles, fewer binding sites would remain free to bind to the 5-FAM(DA)$_3$ probe competing for the same sites. Indeed, a significant decrease in the binding sites available for the 5-FAM(DA)$_3$ was observed after incubation of the particles with the bacteria (Supporting Information Figure S6). The relative fraction of the bound peptide decreased 50 and 70% in the cases of PHMBG-PEI-M and PHMBG-M/SiO_2 (t), respectively. This result indicates a strong affinity of the PHMBG-modified paramagnetic particles for the PG components of the bacterial walls.

The Gram-positive bacteria binding was further characterized by a direct assay of *S. aureus* removal from the suspensions by magnetocollection (for details, see the Experimental Section). As seen in Figure 6, the capture efficiency of the particles depended on their initial concentration, but even with the particle concentration of 0.1 mg/mL the efficiency exceeded 50% in all cases, with

(27) Han, D. H.; Wang, J. P.; Luo, H. L. *J. Magn. Magn. Mater.* **1994**, *136*, 176–182.
(28) Sharif, S.; Kim, S. J.; Labischinski, H.; Schaefer, J. *Biochemistry* **2009**, *48*, 3100–3108.
(29) Fisher, J. F.; Mobashery, S. *J. Med. Chem.* **2010**, *53*, 4813–4829.

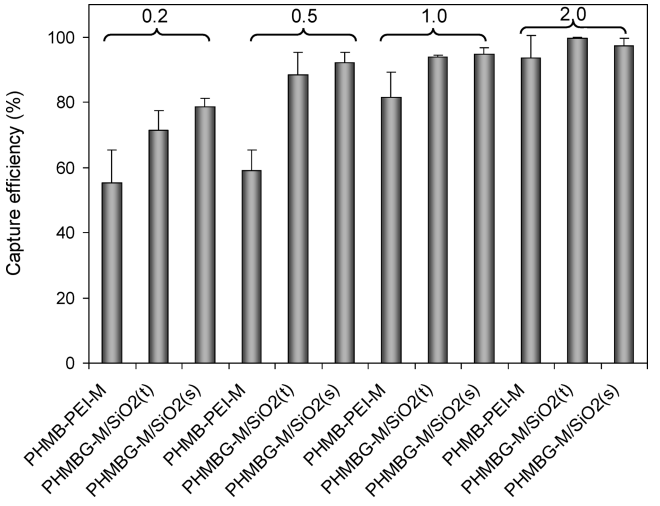

Figure 6. Efficiency of *S. aureus* capture by PHMBG-modified paramagnetic particles at pH 7.4. Numbers stand for initial effective particle concentration in mg/mL. For measurement details, see the Experimental Section.

PHMBG-M/SiO_2 particles reaching 98−99%. The encapsulated PHMBG-M/SiO_2 particles were more efficient in the removal of *S. aureus* than their nonencapsulated counterparts at all particle concentrations, probably due to the higher saturation magnetization that increased the efficiency of magnetocollection. At lower concentrations, the PHMBG-M/SiO_2(s) particles with smaller average diameter were discernibly more efficient than larger PHMBG-M/SiO_2 (t) in capturing and removing the cells, probably due to the higher surface area (and thus the greater number of available PHMBG chains) per particle weight. The particle size appeared to play a significant role in the ability of the particles to kill bacteria.

We also explored the ability of the particles to move to the Gram-positive bacteria cells, as described before.[10] All tested particle fractions moved rapidly under strong magnetic fields and could be delivered to small areas where the bacteria had been located. *S. aureus* were incubated in a Petri dish and allowed to adhere to the center of the bottom of the dish for 8 h. A strong NdFeB magnet (5 × 5 × 5 mm) was placed under the center of the Petri dish followed by the addition of particles. The resulting particle concentration in the dish was 0.1 wt %. With gentle agitation, the particles were attracted to the center of the Petri dish by the magnetic field, where they killed the bacteria. These experiments demonstrated the possibility of directing and manipulating the particles by magnets, which might be useful in such applications as the clearing of tanks, pipes, and other reservoirs with hard-to-reach areas.

Bactericidal Properties of the Nanoparticles. For testing the antiseptic properties of our particles, we chose five Gram-positive and three Gram-negative bacteria that represent a wide range of waterborne microorganisms, all of which are pathogenic with the exception of *L. lactis*, which is extensively used in buttermilk and cheese production. Gram-positive *S. aureus* and *S. epidermidis* are well-known human pathogens, *S. phocae* is a fish and seal pathogen, and *L. garvieae* causes septicemic infections of fish and is the main risk factor for the Mediterranean European trout industry.[30,31] A broth microdilution assay was carried out, and the MIC was determined as the lowest additive concentration that completely inhibited the growth of the bacteria after a 24 h incubation. We tested both PHMBG-M/SiO_2 (t) and PHMBG-M/SiO_2 (s) particle species as well as PHMBG solutions and PHMBG-PEI-M particle suspensions. All paramagnetic nanoparticles tested exhibited strong bactericidal properties (Table 1). The MIC values for the PHMBG-PEI-M particles were in the same range as, or in the case of *S. epidermidis*, much lower than those of the PHMBG polymer, an industrial antiseptic.[32] Of note, we discovered significant differences in the MIC of the PHMBG-M/SiO_2 particles, depending on their average size. The PHMBG-M/SiO_2 (t) particles, which contained particles in the broad range of sizes from ~100 nm up to 0.5 mm, were several-fold (up to 30-fold in the case of *P. aeruginosa*) less effective as bactericides than their PHMBG-M/SiO_2 (s) counterparts sized below ~250 nm (see Figure 2 and Supporting Information Figure S5), despite very similar chemical compositions. The average size of the PHMBG-M/SiO_2 particles affected the diameter of the inhibition zones with the particles in the disk diffusion assay (Supporting Information Figure S7 and Table S1). These observations are in accord with our previous results on the effect of the particle size on the PHMBG-modified particle binding to lipopolysaccharides of the *E. coli* membranes.[10] That is, the PHMBG-PEI-M fraction composed of particles < 50 nm in size was 2−3-fold more efficient in binding and killing *E. coli* than larger particles of identical chemical composition, suggesting better accessibility of the cationic groups on the smaller particles for binding *E. coli* membranes, due to the higher surface area/volume ratio. A similar rationale can be invoked to explain the much higher efficiency of the smaller PHMBG-M/SiO_2 particles against Gram-positive bacteria in the present work, except for the fact that the particles probably bind to peptidoglycan carboxyls exposed to the bacteria membrane exterior in these bacteria. It has been shown that *S. aureus* is strongly negatively charged at neutral pH.[33]

Interestingly, while *L. lactis* was sufficiently susceptible to PHMBG, PHMBG-M/SiO_2(s), and PHMBG-PEI-M nanoparticles, another *Lactococcus* species, *L. garvieae,* did not show comparable susceptibility. Although physiologic characteristics of *L. lactis* and *L. garvieae* are difficult to distinguish, the differences in their susceptibilities to antibiotics are known.[34] It appears that in the present work we discovered susceptibility toward PHMBG-modified nanoparticles as another differentiating feature between these two pathogenic *Lactococcus* species.

Particle Biocompatibility. Since our nanoparticles can come in contact with mammalian cells when they are deployed in the environment as antiseptics, we tested the particles for their potential

Table 1. Minimum Inhibition Concentrations (MIC), in μg/mL, for Aqueous PHMBG Solutions and Dispersions of PHMBG-PEI-M and PHMBG-M/SiO_2 Particles

microorganism (Gram-positive or negative)	PHMBG	PHMBG-PEI-M	PHMBG-M/SiO_2(t)	PHMBG-M/SiO_2(s)
S. aureus (+)	5	35	200	40
S. epidermidis (+)	0.5	0.005	200	15
S. phocae (+)	1.6	1.6	200	15
L. garvieae (+)	40	500	1000	n.a.[a]
L. lactis (+)	20	25	200	25
E. coli (−)	5	5	50	15
S. enterica (−)	110	125	300	120
P. aeruginosa (−)	30	40	1000	30

[a] n.a.: Not available.

(30) Eyngor, M.; Zlotkin, A.; Ghittino, C.; Prearo, M.; Douet, D. G.; Chilmonczyk, S.; Eldar, A. *Appl. Environ. Microbiol.* **2004**, *70*, 5132–5137.
(31) Ravelo, C.; Magariños, B.; López-Romalde, S.; Toranzo, A. E.; Romalde, L. R. *J. Clin. Microbiol.* **2003**, *41*, 751–756.
(32) Kawabata, A.; Taylor, J.A.. *Carbohydr. Polym.* **2007**, *67*, 375–389.
(33) Saggers, B. A.; Lawson, D. *J. Clin. Path.* **1970**, *23*, 262–265.
(34) Elliott, J. A.; Facklam, R. R. *J. Clin. Microbiol.* **1996**, *34*, 1296–1298.

Table 2. Concentration of Additives Allowing for 50% Survival of Mouse Fibroblast Cells (IC_{50}), Mean Concentration of Additives Corresponding to Three-log_{10} Reduction of *S. aureus* (C_{3rf}), and Biocompatibility Index (BI) of PHMBG, PHMBG-PEI-M, and Core−Shell PHMBG-M/SiO_2 Paramagnetic Particles

species	IC_{50} (μg/mL)	C_{3rf} (μg/mL)	BI = IC_{50}/C_{3rf}
PHMBG	170 ± 40	15	11
PHMBG-PEI-M	350 ± 60	13	27
PHMBG-M/SiO2 (t)	2400 ± 130	150	16
PHMBG-M/SiO2 (s)	2100 ± 90	10	210

toxic effects in vitro. We were primarily interested in addressing whether bactericidal concentrations of our nanoparticles would exceed their cytotoxic levels. MTT tests that yield an IC_{50} value, defined as the concentration allowing 50% survival of cells with mouse fibroblasts, are standard tests for cytotoxicity evaluation of various materials[35−37] and thus were used in the present work. The IC_{50} values were compared with the concentration of the microbicidal agents causing a three-log_{10} (99.9%) reduction of the bacteria concentration (C_{3rf}), the minimum acceptable efficacy in the presence of organic matter.[37] The ratio of the IC_{50} and the biocide concentration causing three-log reduction in bacteria count can serve as a relative "biocompatibility index" (BI = IC_{50}/C_{3rf}), which is a measure of the antiseptic agent suitability.[12] The results of these tests are collected in Table 2. It is interesting to observe that the encapsulated particles showed a dramatically (over 10-fold) higher IC_{50} with the fibroblast cells, indicating the lack of toxicity. Yet, the PHMBG-M/SiO_2 particles were bactericidal, with the smaller fraction of the particles having C_{3rf} similar to or lower than the analogous value for the PHMBG solution or PHMBG-PEI-M particles. The lower toxicity of the encapsulated particles yielded the higher BI values. It is difficult to provide an explanation of the biocompatibility of the PHMBG-M/SiO_2 particles at present, but the discovered compatibility combined with the high chemical and structural stability of the particles and the relative ease of synthesis afford a nanoparticle-based platform for novel antiseptics.

Concluding Remarks

The paramagnetic nanoparticles presented here are capable of strong attraction to bacterial membranes, affording a capability of binding the microorganisms to the particles and the subsequent bacteria capture, manipulation, and recovery by means of a magnet. The interaction between the PHMBG-decorated particles and Gram-positive bacterial membranes is evidently dominated by the electrostatic attraction between the polycationic particle and the negative charge of the D-alanyl-D-alanine residues exposed on the exterior surface of the bacteria. Furthermore, we expect that there are hydrogen bonding interactions between the carbonyl oxygens of the D-Ala residues and the amino/imino hydrogen bond donors of the PHMBG segments, along with the hydrophobic contacts of the hexamethylene groups of PHMBG with the methyl side chains of the D-Ala residues (Figure 7). These attractive interactions are analogous to those between *S. aureus* membranes and vancomycin and other antibiotics, which are well-studied.[38−40]

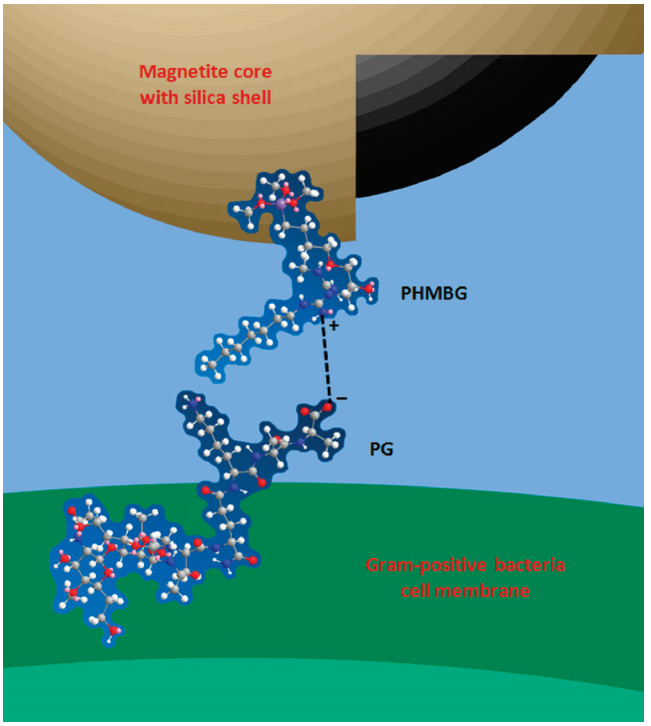

Figure 7. Cartoon depicting interactions between a PHMBG segment attached to the polysiloxane shell of the core-shell paramagnetic particle and an L-Lys-D-Ala-D-Ala segment of the peptidoglycan (PG) on the surface of a Gram-positive bacterium. Color code: white (hydrogen), red (oxygen), gray (carbon), blue (nitrogen), purple (silicon), and pink (lone pair of electrons). The molecular structures were energy-minimized using Molecular Modeling Pro (Norgwyn Montgomery Software Inc.).

Our particles are nonselective and capture both Gram-positive and Gram-negative bacteria, as the electrostatic and hydrophobic attractions are nonspecific, compared to the hydrogen bond formation between nanoparticles modified with vancomycin and Gram-positive bacteria.[6,8] Nevertheless, our nonspecific particles possess a broad-range bactericidal activity and thus can act as "recoverable antiseptics" capable of long-term presence in aqueous reservoirs. In terms of monitoring, methods to analyze captured nucleic acids need to be developed to enable the selective detection of DNA of targeted germs, rather than large excesses of nontargeted nucleic acid material that the particles are able to capture. The means of detection have been discussed previously.[12] In the present work, we concentrated on the core-shell particles, which were synthesized by the encapsulation of the magnetite core by a functional silane followed by the formation of a polysiloxane shell. The encapsulation dramatically enhances the chemical stability and saturation magnetization of the magnetite compared to the nonencapsulated particles, where a direct complexation between magnetite and amine-containing polymers is permitted. We also discovered that the encapsulated particles possess high biocompatibility with mammalian cells.

Acknowledgment. The authors were supported, in part, by the Defense Threat Reduction Agency Grant HDTR1-09-1-0012. The support by FEDER and MICINN (SAF2008-01679) of Spain is gratefully acknowledged.

Supporting Information Available: Kinetics of the binding of 5-FAM$(DA)_3$ to the PHMBG-PEI-M particles, TEM image of magnetite nanoparticles stabilized by TMAOH, TEM image

(35) ASTM F813, Standard practice for direct contact cell culture evaluation of materials for medical devices. *Annual Book of ASTM Standards 13.01*; ASTM: Philadelphia, 1987.
(36) Müller, G.; Kramer, A. *J. Antimicrob. Chemother.* **2008**, *61*, 1281–1287.
(37) Pitten, F. A.; Werner, H. P.; Kramer, A. *J. Hosp. Infect.* **2003**, *55*, 108–115.
(38) Liu, S.; Chang, J. S.; Herberg, J. T.; Horng, M.-M.; Tomich, P. K.; Lin, A. H.; Marotti, K. R. *Proc. Natl. Acad. Sci.U.S.A.* **2006**, *103*, 15178–15183.
(39) Leung, S. S. F.; Tirado-Rives, J.; Jorgensen, W. L. *Bioorg. Med. Chem.* **2009**, *17*, 5874–5886.
(40) Kim, S. J.; Cegelski, L.; Preobrazhenskaya, M.; Schaefer, J. *Biochemistry.* **2006**, *45*, 5235–5250.

of magnetite nanoparticles encapsulated by TEOS and GPTMS, FTIR spectra of bare magnetite, GPTMS, and magnetite encapsulated by GPTMS and TEOS, number-average hydrodynamic diameter of PHMBG-M/SiO2 (s) and PHMBG-PEI-M particles, binding of 5-FAM$(DA)_3$ onto paramagnetic particles before and after incubation with *S. aureus*, photographs of inhibition zones observed for the discs containing PHMBG-PEI-M or PHMBG in Petri dishes cultured with bacteria, diameter (in mm) of the inhibition zones observed using the disk diffusion susceptibility test. This material is available free of charge via the Internet at http://pubs.acs.org.